AD-A010 802

STUDY OF THE ELECTRONIC SURFACE STATE OF III-V COMPOUNDS

W. E. Spicer

Stanford University

Prepared for:

Army Electronics Command
Defense Advanced Research Projects Agency

15 October 1974

DISTRIBUTED BY:

NTIS

National Technical Information Service
U. S. DEPARTMENT OF COMMERCE

171174

ADA010802

STUDY OF THE ELECTRONIC SURFACE STATE OF III-V COMPOUNDS

SEMI-ANNUAL TECHNICAL PROGRESS REPORT

W. E. Spicer, Principal Investigator

15 October 1974

NIGHT VISION LABORATORY
U. S. Army Electronics Command
Fort Belvoir, Virginia 22060

Sponsored by

DEFENSE ADVANCED RESEARCH PROJECTS AGENCY
DARPA ORDER NO. 2182
PROGRAM CODE NO. 4D10
CONTRACT NO. DAAK02-74-C-0069

Effective: 1973 September 01   Expiration: 1975 August 31

The views and conclusions contained in this document are those of the author and should not be interpreted as necessarily representing the official policies, either expressed or implied, of the Defense Advanced Research Projects Agency of the U. S. Government.

Reproduced by
NATIONAL TECHNICAL
INFORMATION SERVICE
US Department of Commerce
Springfield, VA. 22151

SOLID-STATE ELECTRONICS LABORATORY
STANFORD ELECTRONICS LABORATORIES
STANFORD UNIVERSITY · STANFORD, CALIFORNIA

STUDY OF THE ELECTRONIC SURFACE STATE OF III - V COMPOUNDS

SEMI-ANNUAL TECHNICAL PROGRESS REPORT

W. E. Spicer, Principal Investigator

Telephone: (415) 497-4643

15 October 1974

NIGHT VISION LABORATORY
U. S. Army Electronics Command
Fort Belvoir, Virginia 22060

Sponsored by

DEFENSE ADVANCED RESEARCH PROJECTS AGENCY
DARPA ORDER NO. 2182
PROGRAM CODE NO. 4D10

CONTRACT NO. DAAK02-74-C-0069

Effective: 1973 September 01 Expiration: 1974 August 31 $88,573

STANFORD ELECTRONICS LABORATORIES
STANFORD UNIVERSITY
STANFORD CALIFORNIA 94305

The views and conclusions contained in this document are those of the authors and should not be interpreted as necessarily representing the official policies, either expressed or implied, of the Defense Advanced Research Projects Agency of the U. S. Government.

SUMMARY

In the past six months work has proceeded on studies of bulk cesium oxide, and the surface of GaAs and GaSb. The overall aim of these studies is to provide a basic understanding of the surfaces of the materials used in III-V photocathodes.

We have oxidized bulk cesium metal and find that for low oxygen exposures the surface appears to stay metallic while $O^{=}$ ions dissolve in the bulk of the cesium. With oxidation the work function drops to a minimum of about 0.7 eV. Further oxidation raises the work function.

We found that oxidation of p type GaAs causes the bands to bend down about 0.5 eV at the surface.

Our work on GaSb indicates that there are neither empty nor filled surface states in the band gap.

TABLE OF CONTENTS

	Page No.
I. CESIUM OXIDE	
Introduction	3
Experimental Details	3
Results	
A. Introduction	5
B. Low Oxygen Exposure (Regions I and II	5
C. Regions of Large Oxygen Exposure (Regions II, III, IV)	7
II. GaSb	8
III. GaAs	10
Figures	
1. Diagram of experimental setup for cesium oxide experiment.	14
2a. Yield of cesium oxide versus oxygen exposure.	15
2b. Work function of cesium oxide versus oxygen exposure.	16
3. EDCs of cesium oxide at 7.7 eV for clean cesium through 30L oxygen exposure.	17
4. EDCs of cesium oxide at 7.7 eV for oxygen exposure from 30L to 200L.	18
5. EDCs of cesium oxide at 7.7 eV for oxygen exposure from 200L to 1000L.	19
6. EDCs of cesium oxide at 7.7 eV for oxygen exposure from 1000L to 40,000L.	20

TABLE OF CONTENTS CON'T.

		Page No.
7.	EDCs of cesium oxide at 10.2 eV for oxygen exposure for clean cesium through 30L oxygen exposure.	21
8.	EDCs of cesium oxide at 10.2 eV for oxygen exposures from 200L to 1000L.	22
9.	EDCs of cesium oxide at 10.2 eV for oxygen exposures from 200L to 1000L.	23
10.	EDCs of cesium oxide at 10.2 eV for oxygen exposures from 1000L to 40,000L.	24
11.	EDCs of clean n type GaSb.	25
12.	EDCs of n type GaSb at 10.2 eV for several oxygen exposures.	26
13.	EDCs of clean p type GaSb.	27
14.	EDCs of p type GaSb at 10.2 eV for several oxygen exposures.	28
15.	EDCs of clean n and p type GaSb at 10.2 eV.	29
16.	EDCs of p type GaAs for several oxygen exposures.	30
17.	EDCs of n type GaAs for several oxygen exposures.	31
18.	EDCs of n and p type GaAs at 11.6 eV.	32
19.	Position of Fermi level at the surface versus oxygen exposure for GaAs and Si .	33

I. CESIUM OXIDE

INTRODUCTION

Instabilities in the cesium oxide surface layers have been a serious problem for 1.06 μ photoemitters. The object of the work reported here is to obtain information on bulk cesium oxides and then to make correlations between it and ultraviolet photoemission data which will be obtained from cesium oxides on actual cathodes.

In particular, it is well known that details of valence band structure associated with various compounds can be obtained from photoemission energy distribution curves (EDCs). Conversely, to identify production of different compounds we plan to use changes in EDCs as the oxidation of Cs proceeds. The next step will be to take EDCs from the cesium oxide on III-V compound photoemitters and to see if the same surface species can be identified. By changing the cesium to oxygen ratios we hope to establish whether or not the instabilities can be associated with changes in the cesium compounds that form thin cesium oxide layers on photo-cathodes. In this work we have profited very much from discussions with Ron Bell and John Edgecomb of Varian.

EXPERIMENTAL DETAILS

The experiment was carried out in a stainless steel ultra-high vacuum system with a base pressure of about 3×10^{-10} Torr as measured on a Redhead gauge. EDCs were measured using a standard retarding potential system.[1]

The cesium metal was contained in a vacuum sealed glass ampul. The ampul contained about 1/3 gram of Cs which had been vacuum distilled from a 1 gram Cs ampul purchased from Electronic Space Products, Inc.

The 1/3 gram ampul was placed in a copper side arm of about 30 cm total length, as shown in Fig. 1. After pump down and bakeout of the system the side arm was crushed to break the ampul. The Cs remained in the side arm after the ampul was crushed. It was necessary to heat the side arm with heat tapes or a propane torch in order to evaporate cesium at a sufficiently rapid rate.

The cesium was evaporated onto a copper substrate which had been cooled to approximately 140 K with a liquid nitrogen cooled cold strap (see Fig. 1). After several hours of cooling the substrate temperature reached a minimum of 100 K. All data shown in this article was measured at a temperature between 100 K and 140 K on films which had never been warmed above 140 K.

It took approximately one hour to evaporate a sample sufficiently thick for measurements. It was not possible to measure the thickness of the cesium layer, but it was visible as a dull, dark layer on the substrate. A white-green layer of Cs , apparently much thicker than that on the substrate, formed on the cold strap. During evaporation the yield was monitored at 7.7 eV. The yield first rose as a monolayer of Cs was deposited, and then fell as a bulk Cs layer formed.

During Cs evaporation the pressure rose to about 5×10^{-8} Torr. During measurement the pressure was approximately 3×10^{-9} Torr. The system was pumped by an Orb-Ion pump and a small VacIon. It was necessary to turn the Orb-Ion off during measurements because the light from its filaments caused photoemission from the Cs .

The Cs was oxidized while cold by admitting high purity (10 ppm impurities) oxygen into the system through a Varian leak valve.

The presence of Cs in the system caused large reverse currents, which produced low energy peaks in the EDCs, similar to those shown in Fig. 1 of Reference 2. The reverse current peaks have been removed from the EDCs shown in this paper.

The Cs also lowered the emitter to ground resistance to only about 10^{8} ohms. We were not able to raise the resistance by heating the emitter. This low resistance made it impossible to take EDCs at photon energies for which the forward current was below 10^{-10} amps.

RESULTS

A. Introduction

Figure 2a shows the photoelectric yield of the oxidized cesium film as a function of oxygen exposure. From it we see that the oxidation process up to 4×10^{4} Langmuirs ($1L = 10^{-6}$ Torr-second) may be divided approximately into four regions. In region I there is only a slight increase in yield with exposure. At about 10L a more rapid rate of increase is observed, up to about 100L, at which point the yield begins to rise rapidly. At 500L we enter region IV where the yield drops slowly with exposure.

EDCs of oxidized cesium are shown in Figs. 3 through 10. Two sets of EDCs are presented for $h\nu = 7.7$ and $h\nu = 10.2$ eV. The EDCs shown are taken from two different runs of the experiment. The EDCs were quite reproducible from the two runs. The EDCs are normalized so that the area under the curve equals the yield at that photon energy. Note that there is a scale charge between Figs. 3 and 4, 4 and 5, 7 and 8, and 8 and 9.

B. Low Oxygen Exposure (Regions I and II)

EDCs for clean Cs are shown in the bottom curves in Figs. 3 and 7. Peak A is due to unscattered electrons from the Cs valence band. These

EDCs agree very well with previous work on clean Cs [2,3] except that the weak structure labeled B_1 in our curves is much weaker than the peak in the same position in the work of Smith et al. Since shoulder B_1 is at the same location where the strong oxide peak B develops, we believe that the clean Cs investigated by Smith actually had a small oxygen contamination. Our curve for 1L exposure looks more like the EDCs of Smith than our EDCs from clean Cs . We believe that our Cs was very clean because the Cs was distilled under vacuum once before the ampul was placed in the experimental chamber, and because the long path around two bends which the Cs had to traverse on its way to the substrate (see Figure 1) caused further purification of the Cs . On the other hand, Smith's apparatus featured a line-of-sight evaporation from the Cs ampul to the substrate.

Peak B_1 has previously been attributed to valence electrons which have been scattered by a surface plasmon.[2,3] Our data does not preclude that explanation; we still see a weak shoulder B_1 before oxidation. The shoulder is fairly broad compared to the oxide peak B , which tends to suggest that the shoulder B_1 is not caused by oxygen contamination. The shoulder could be caused by the surface plasmon as originally proposed, or it could be due to small quantities of contaminents in the Cs .

In Figs. 3 and 4 it is important to note that the magnitude of peak A deos not decrease for oxygen exposures up to 200L, although the growth of structure below -2 eV is very dramatic. Peak A is caused by unscattered electrons emitted from the conduction band of cesium. The growth of oxide emission while the peak characteristic of the metal remains constant is similar to the behavior seen in Sr ,[4] and suggests the same explanation for the Cs-oxidation as for the Sr oxidation.

In the Sr work it was found that, until oxidation neared completion, the oxide was located beneath the surface. The first step in the oxidation process was the appearance of dissolved $O^=$ ions below the surface. The first step in the oxidation of Cs appears to be identical to that of Sr, i.e., $O^=$ ions are dissolved in the Cs metal. This is followed by precipitation of crystallites. Here Sr differs from Cs in that it has one dominant oxide whereas Cs has many oxides. Thus we believe that at least up to the 200L exposure, there is a layer of Cs metal on the surface, with the oxide lying in the bulk of the material.

The extreme sharpness of the peak B for exposures up to 30L is also similar to the behavior of Sr oxidation,[5] and again we believe that the explanation is the same in both cases: for the first 20-30L the oxygen atoms are well separated so that the oxygen-oxygen overlap is very small. Thus the peak B is an atomic-like oxygen level. From 30-100L, peaks C and D develop, indicating that oxygen levels overlap at these exposures, i.e., formation of cesium oxygen compounds starts.

C. Regions of Large Oxygen Exposure (Regions II, III, and IV)

As can be seen from Figs. 4-6 and 8-10, there are very distinct changes in the EDCs as the oxidation proceeds from 30 to 5000L. Based on phase diagrams and estimates of vapor pressure, Ron Bell[5] has estimated that the phase important for activation of photocathodes is Cs_2O_2. Cs_2O_2 and four other compositions lie on the cesium rich side of this composition.

Another important parameter is contained in Figures 3-8. This is the work function $e\varphi$, which is obtained from the EDCs by the difference in magnitude of the low energy cutoff and the photon energy. In Figure 2b the work function is plotted versus oxygen exposure.

At 500L oxygen exposure, the yield (Figure 2a) reaches a maximum and the work function reaches a sharp minimum of about 0.7 eV. In addition a fairly distinct EDC is obtained at 500L. Note in particular that a distinct peak (C) is present at -4.5 eV in Figure 9, which is not well defined for any nearby oxygen exposure. Thus it appears that a fairly distinct EDC occurs for the low work function form of cesium oxide. Our next step will be to obtain EDCs from cesium oxide on GaAs and compare these with the oxides studied in the present work.

II. GaSb

Two GaSb samples, $10^{18}cm^{-3}$ n type (18n) and $10^{17}cm^{-3}$ p (17p), have been studied. The 18n sample was misoriented by the manufacturer along the (111) direction instead of the (110) direction, causing the crystal to cleave at a large angle to the crystal axis. This disrupted the geometry of the retarding potential analyser and reduced its resolution. However, the data obtained from this cleave (Figures 11,12) appears interesting. The manufacturer has supplied a properly oriented replacement for sample 18n at no additional cost. We plan to repeat the measurements of the oxidation of sample 18n, presented below, in the near future on the properly oriented sample. We also will study the effect of Cs on this sample.

The cleave was made at a pressure of 8×10^{-12} Torr. The EDCs showed a tail up to the Fermi level, which was caused by the reduced resolution of the electron energy analyser. No strong emission from filled surface states was observed. Our estimate places the surface Fermi level quite close to the bulk position, that is, near the conduction band

minimum. This indicates that there are no empty surface states in the band-gap. The structure in the EDCs also tended to be broad, which sharpened somewhat with light oxidation (~10^2 L). This may indicate a non-uniform work function across the surface, broadening the structures, and the O_2 removes the non-uniformity. Viljoen et al.[6] observed that the work function of cleaved GaSb varied by as much as 0.6 eV across the surface, and this variation vanished after a few days. Upon oxidation of sample 18n, the Fermi level moved towards the valence band maximum and at 10^4 L the movement was almost half a volt. At exposures greater than 10^4 L the Fermi level moved away from the VBM and after 10^8 L exposure had returned to within 0.3 eV of its original (unoxidized) position. See Fig. 12. The EDC at 10^8 L exposure should be contrasted with the 17p sample at the same exposure (Fig. 14). The 17p sample appears to be at a more advanced stage of oxidation, with a higher peak at about -5 eV. The cleave on sample 17p was very rough because the sample is very brittle and has a tendency to chip rather than to cleave. This brittleness seems to be peculiar to sample 17p; sample 18n cleaved very well even though it was oriented wrong. We cleaved sample 17p only once because of the bad cleave. We will attempt to make changes in the cleaving apparatus which will improve our chances of getting a good cleave before we attempt another cleave on sample 17p.

The 17p data is shown in Figures 13 and 14. The surface Fermi level appears to within experimental accuracy, to be at the bulk position, which is about 0.1 eV above the VBM. This means that there are no strong surface states near the bottom of the energy gap. The oxidation behavior was quite different from the n type's. The structures were sharper in the clean EDCs and the Fermi level showed little movement with oxygen

exposure. The oxygen peak built up more rapidly. The 10^7 L curve looks very much like the 10^8 L curve of the 10^{18} n sample. In Figure 15 we lined up the leading peak for the two different dopings and it can be clearly seen that the positions of the Fermi levels differ by almost the full bandgap. This suggests that the bandgap is free of surface states. Future work will include studies of effects of cesium on the clean surface.

III. GaAs

Since our last report, one additional cleave has been made on our $3 \times 10^{19}\ cm^{-3}$ p type GaAs sample (sample 19p). This sample was exposed to oxygen. EDCs for sample 19p are shown in Figure 16 as a function of oxygen exposure. Exposures up to 10^4 L have little effect on the EDCs. At 10^5 L, the Fermi level begins to move to higher energy relative to the leading peak in the EDC, and by 10^7 L it has moved upward by about 0.5 eV. Also, at about 10^7 L a large oxide peak has built up.

The behavior of a $6 \times 10^{14}\ cm^{-3}$ n type GaAs sample (sample 14n) upon oxidation is shown in Figure 17. The overall shape of the EDCs is similar for the clean and oxidized n and p type samples. Figure 18 compares EDCs for heavily oxidized n and p type GaAs.

However, the behavior of the position of the Fermi level is different for the two samples. On sample 14n the position of the Fermi level is almost constant with oxidation, while the Fermi level moves up on the p type sample. The position of the Fermi level with oxygen exposure is shown at the top of Figure 19. The behavior of the position of the Fermi level on silicon is shown for contrast at the bottom of Figure 19, which is taken from Reference 7.

In silicon, the Fermi level is pinned for both n and p type material. Oxidation destroys the surface states which pin the Fermi level on n type silicon. On p type silicon, the surface states are replaced by Si oxide interface states which pin the Fermi level.

The behavior of GaAs is different than that of Si . The Fermi level is pinned on clean n type GaAs , but not on p type. Oxidation does not affect the pinning on the n type, but oxidation beyond 10^5 L pins the Fermi level on p type GaAs and causes the bands to bend down.

We can explain this behavior in terms of the model of the GaAs (110) surface that we have previously presented.[8] We believe that the oxygen first binds to the As atoms at the surface. The filled surface states are associated with the As surface atoms, and are located below the valence band maximum and do not pin the Fermi level. Thus the first oxygen exposure does not affect the pinning of the surface states. At about 10^5 L exposure, we believe that the As sites are filled, and additional oxygen bonds to surface Ga atoms. Oxygen bonds to the Ga atoms would require breaking Ga-As bonds at the surface, and would thus create interface states. The interface states would then be responsible for the pinning of the Fermi level on the heavily oxidized p type sample.

Work in now in progress on a more lightly doped p type sample (10^{17} cm^{-3}). Before this sample is cleaved, an attempt will be made to heat clean it, as a preliminary experiment to help us prepare for the heat cleaning of faces of GaAs other than the (110) cleavage face. We also plan to study cesium on the surface of this sample to attempt to reproduce the behavior of Cs on sample 19p reported in our previous semiannual report. We

will also attempt to correlate our bulk Cs-oxide studies with Cs-oxide on sample 17p.

We plan to oxidize sample 17p with special attention to carefully studying the behavior between 10^4 L and 10^7 L, the exposure region where the movement of the Fermi level and the change in shape of the EDCs is seen.

REFERENCES

1. C. R. Eden, Ph.D. Thesis, Stanford University (unpublished)
2. N. V. Smith and G. B. Fisher, Phys. Rev. B 3, 3662, (1971).
3. N. V. Smith and W. E. Spicer, Phys. Rev. Lett. 23, 769, (1969).
4. C. R. Helms and W. E. Spicer. Phys. Rev. Lett. 28, 565, (1972); 31, 1307, (1973); 32, 228, (1974); Appl. Phys. Lett. 21, 237, (1972).
5. Ronald Bell, personal communication.
6. P. E. Viljoen, M. S. Jazzar and T. E. Fischer, Surface Sci. 32, 506, (1972).
7. L. F. Wagner and W. E. Spicer, Phys. Rev. B 9, 1512, (1974).
8. P. E. Gregory, W. E. Spicer, S. Ciraci and W. A. Harrison, to be published in Appl. Phys. Lett. 25, (1974).

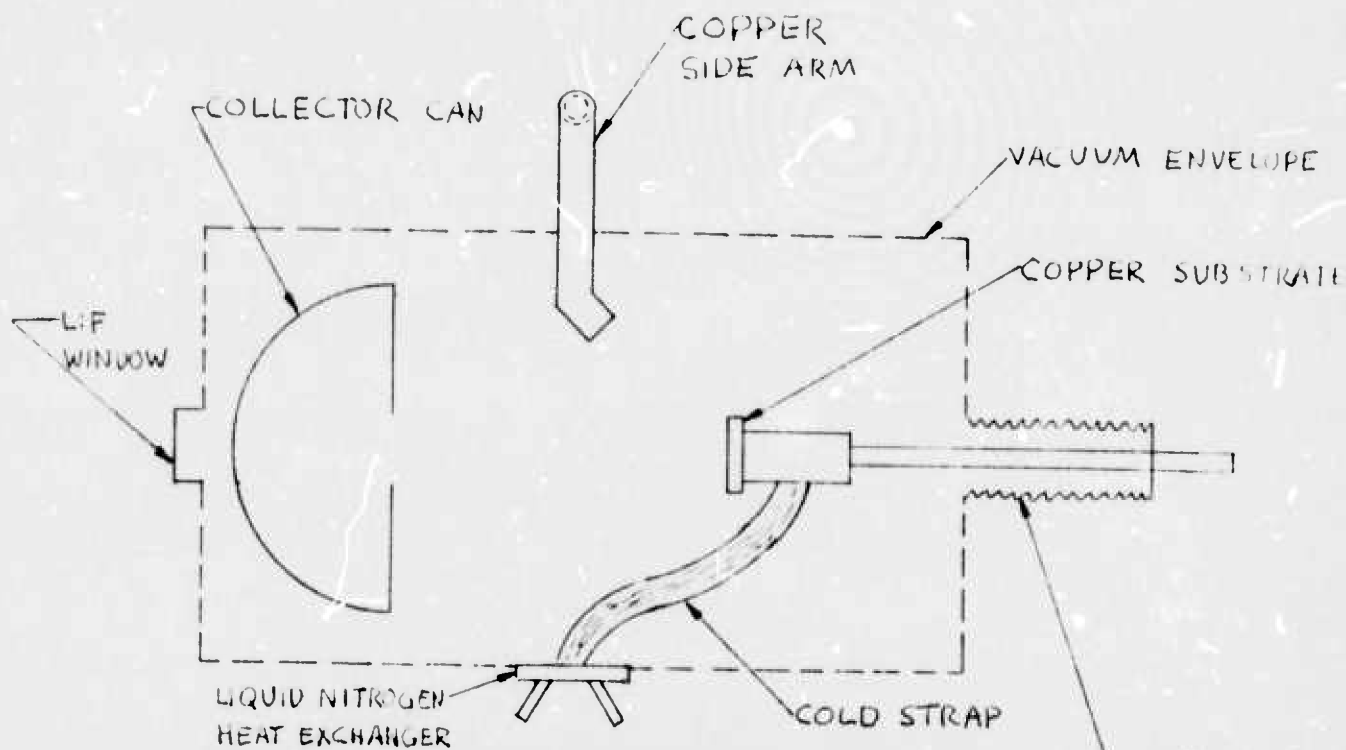

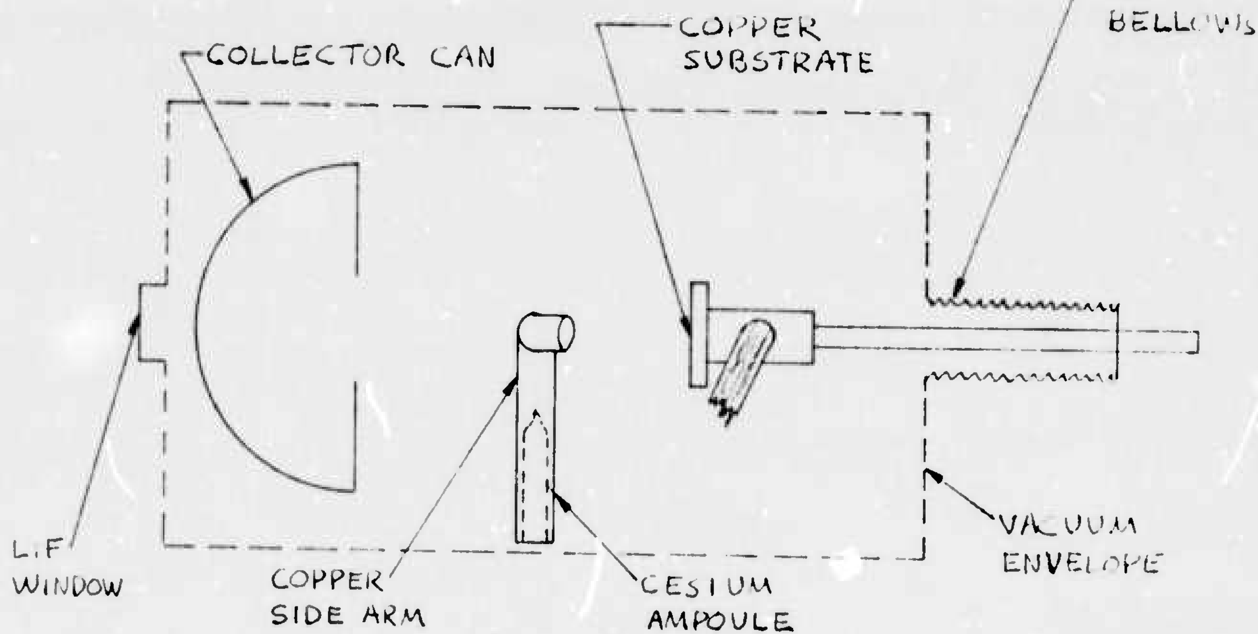

FIGURE 1

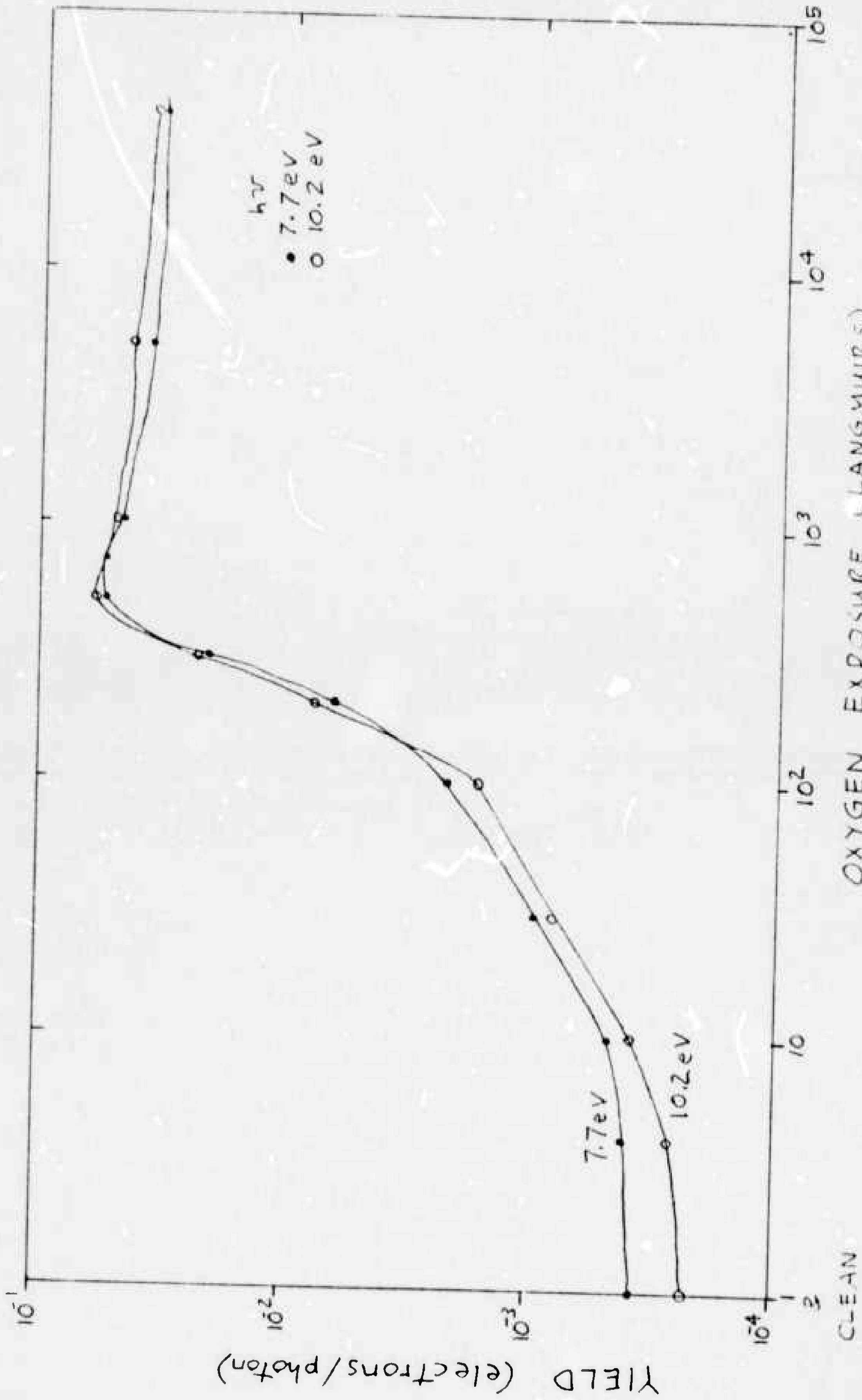

FIGURE [illegible]

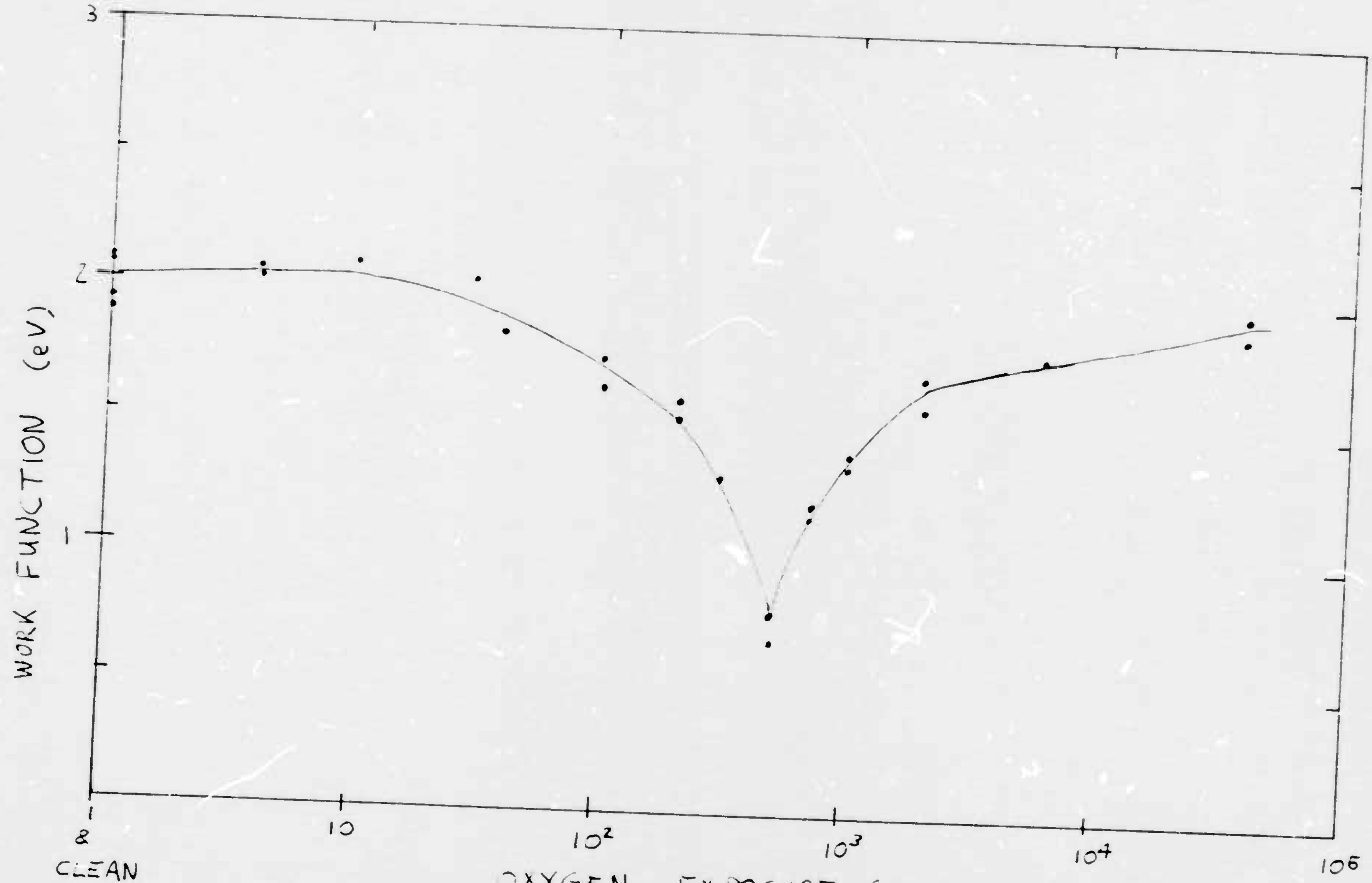

FIGURE 2b

FIGURE 3

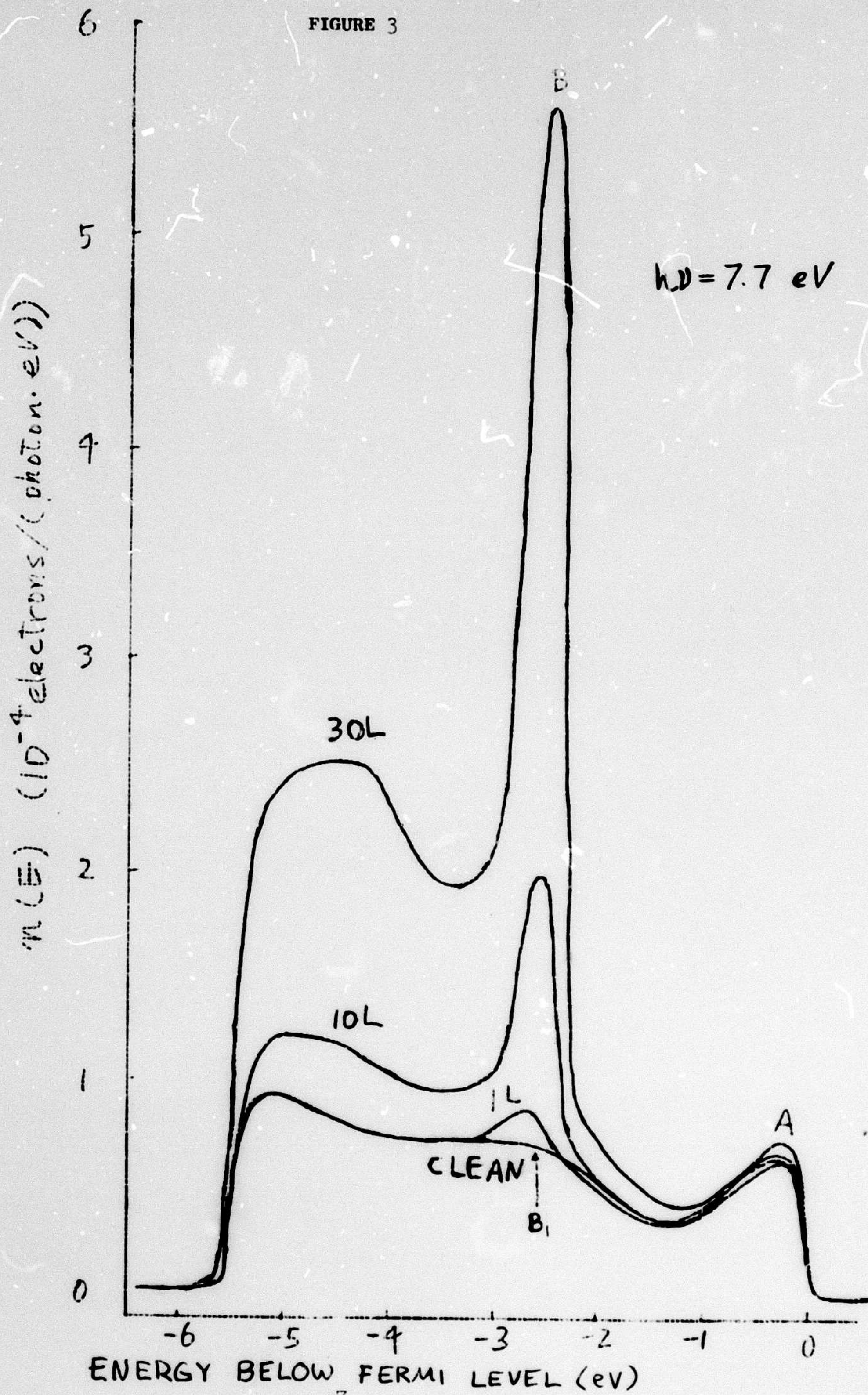

FIGURE 4

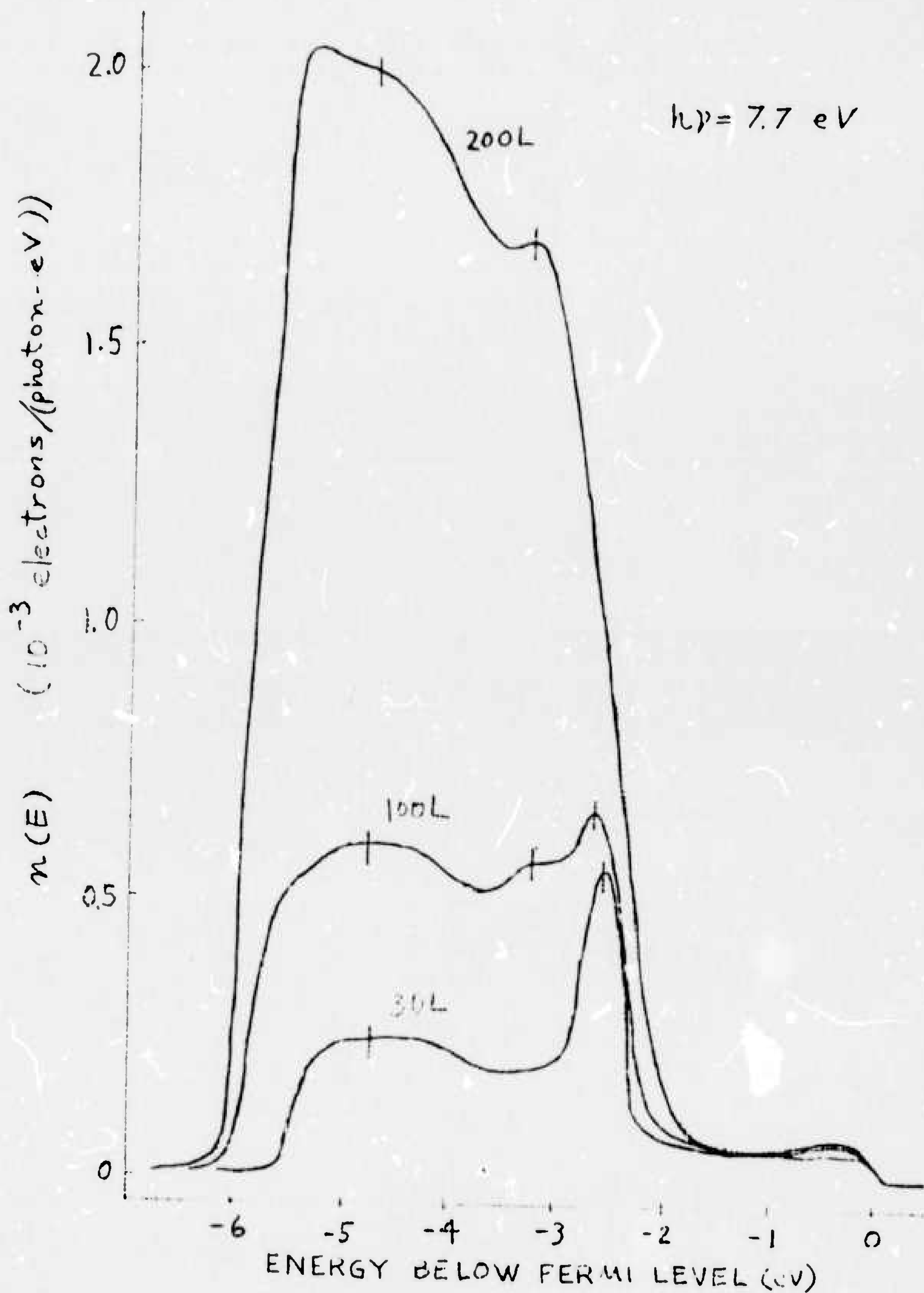

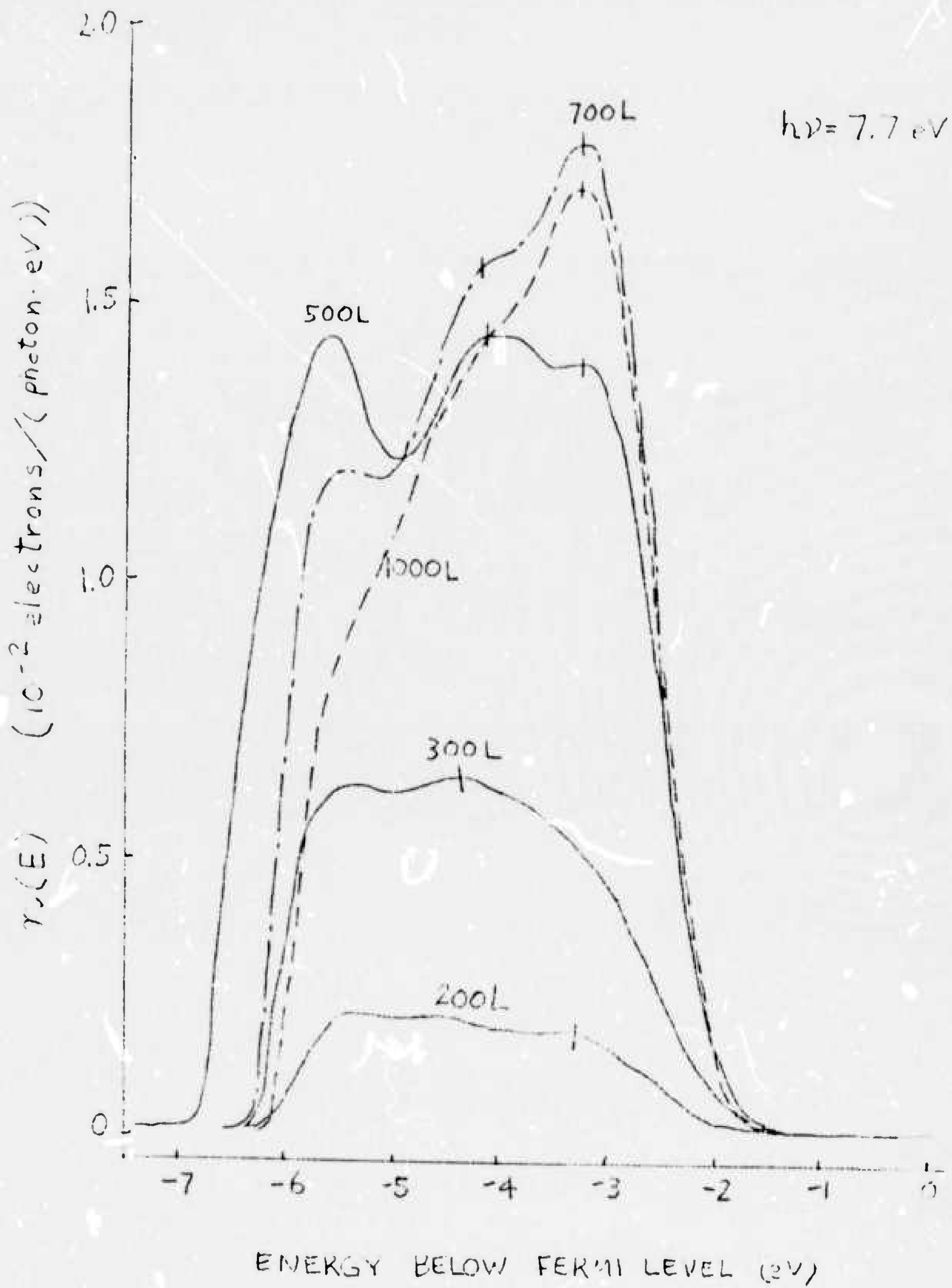

FIGURE 5

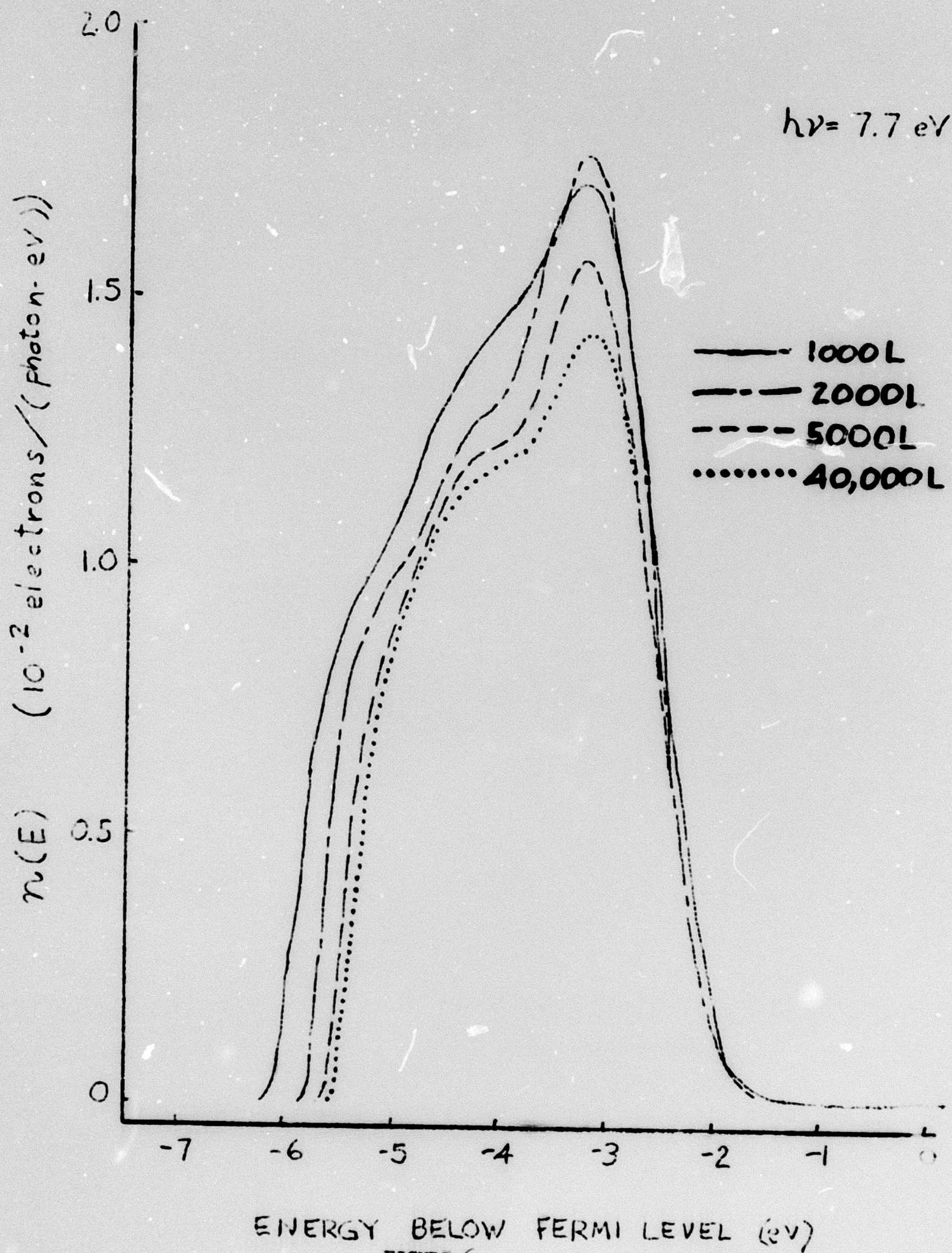

FIGURE 6

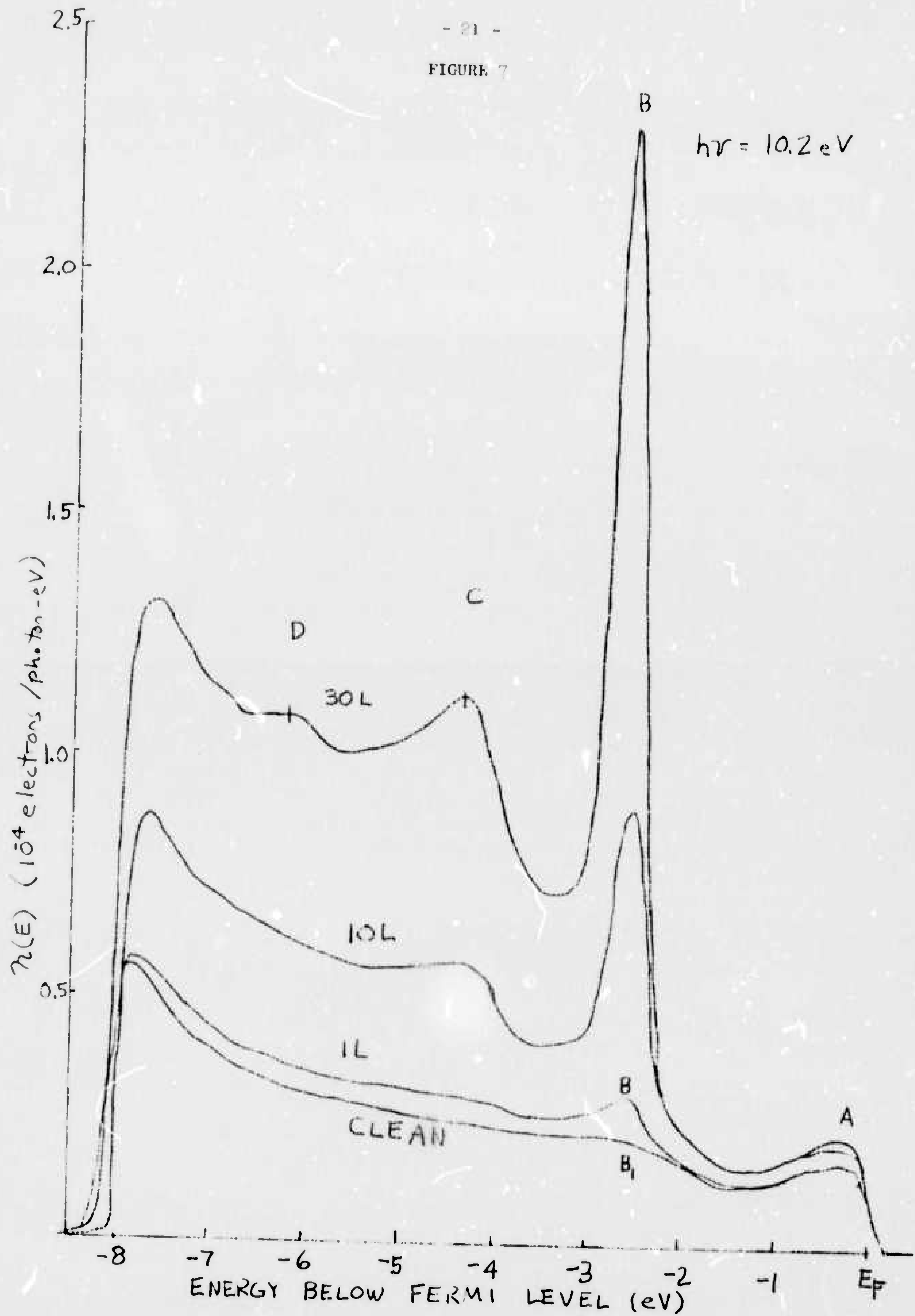

FIGURE 7

FIGURE 8

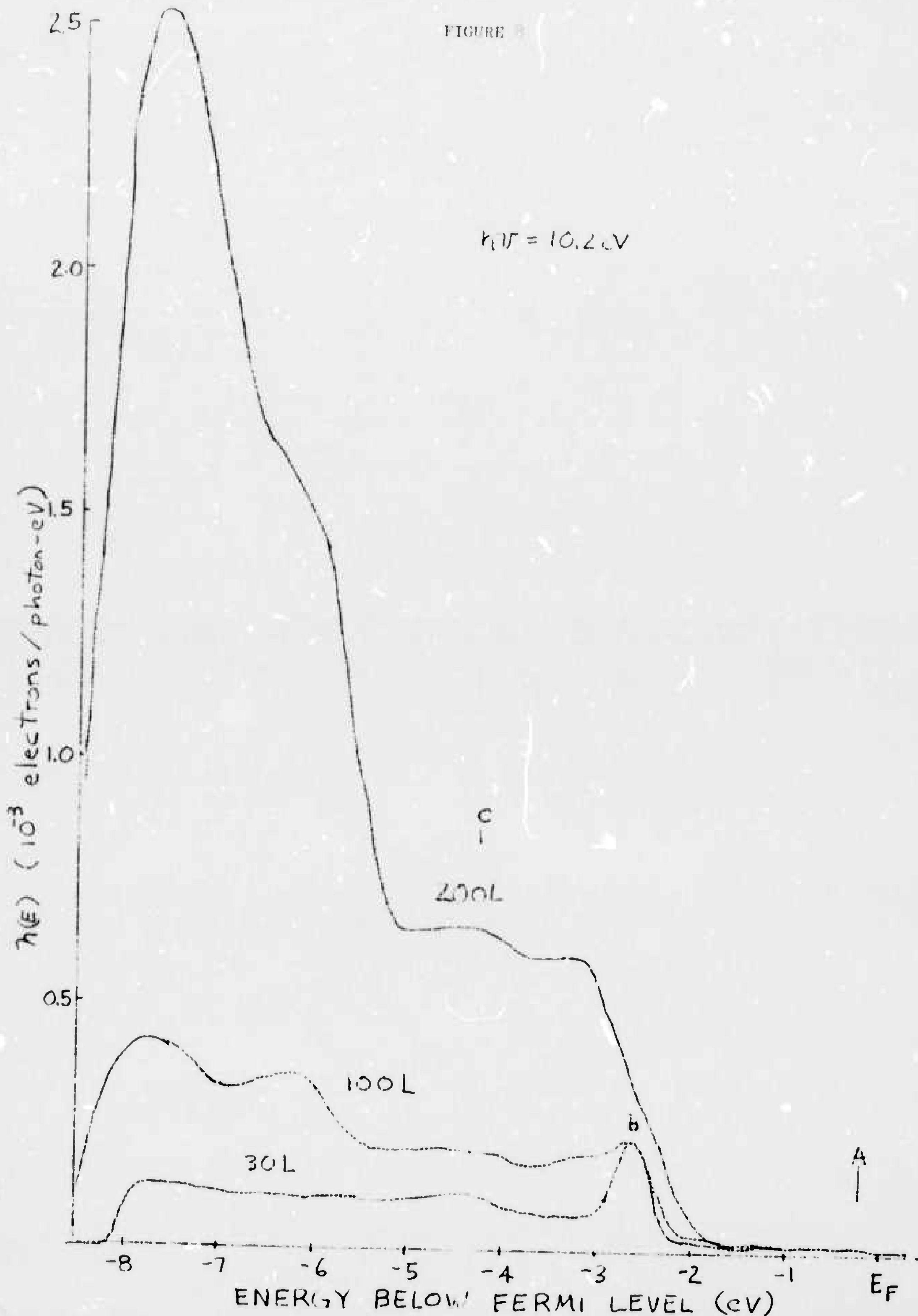

FIGURE 9

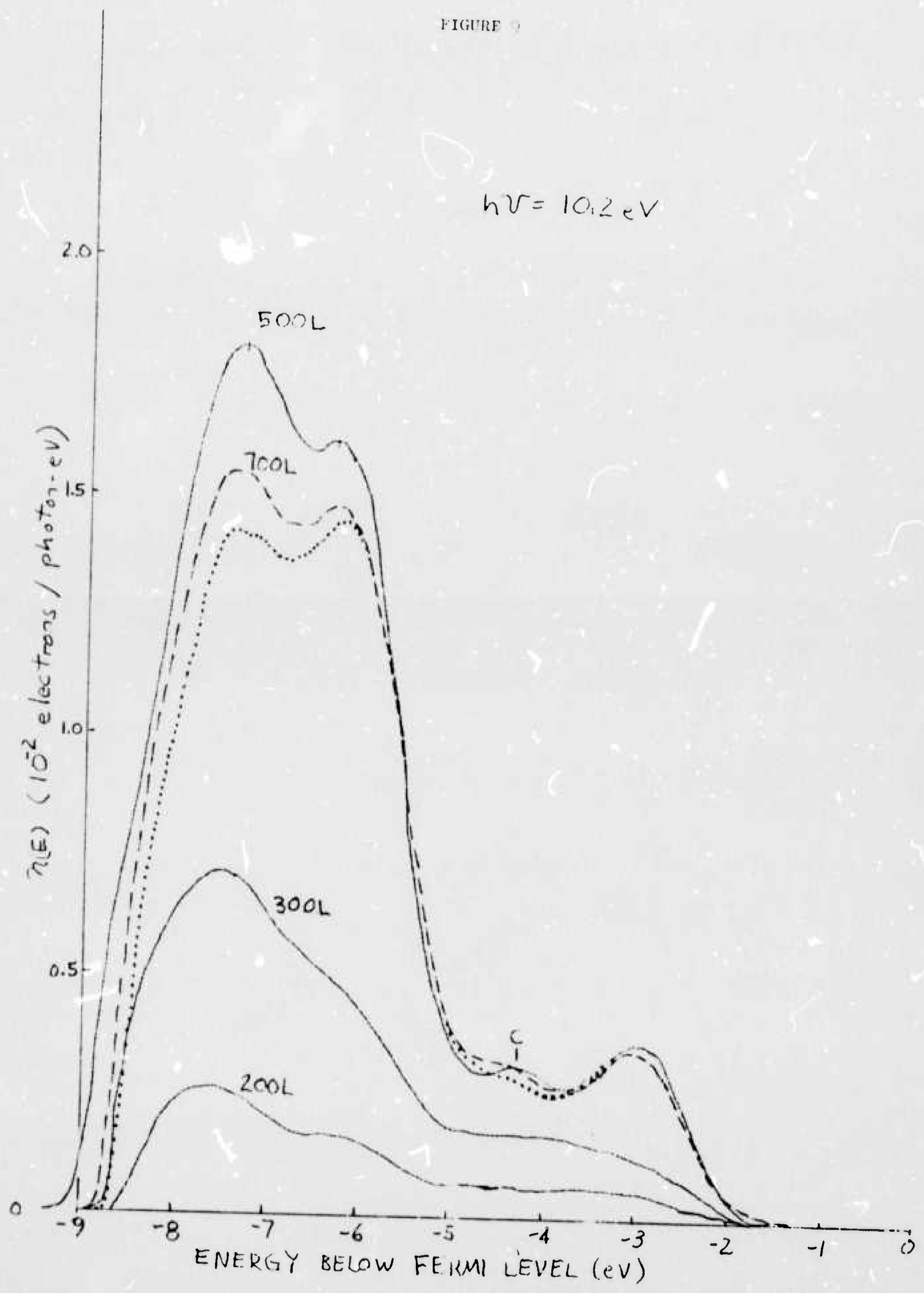

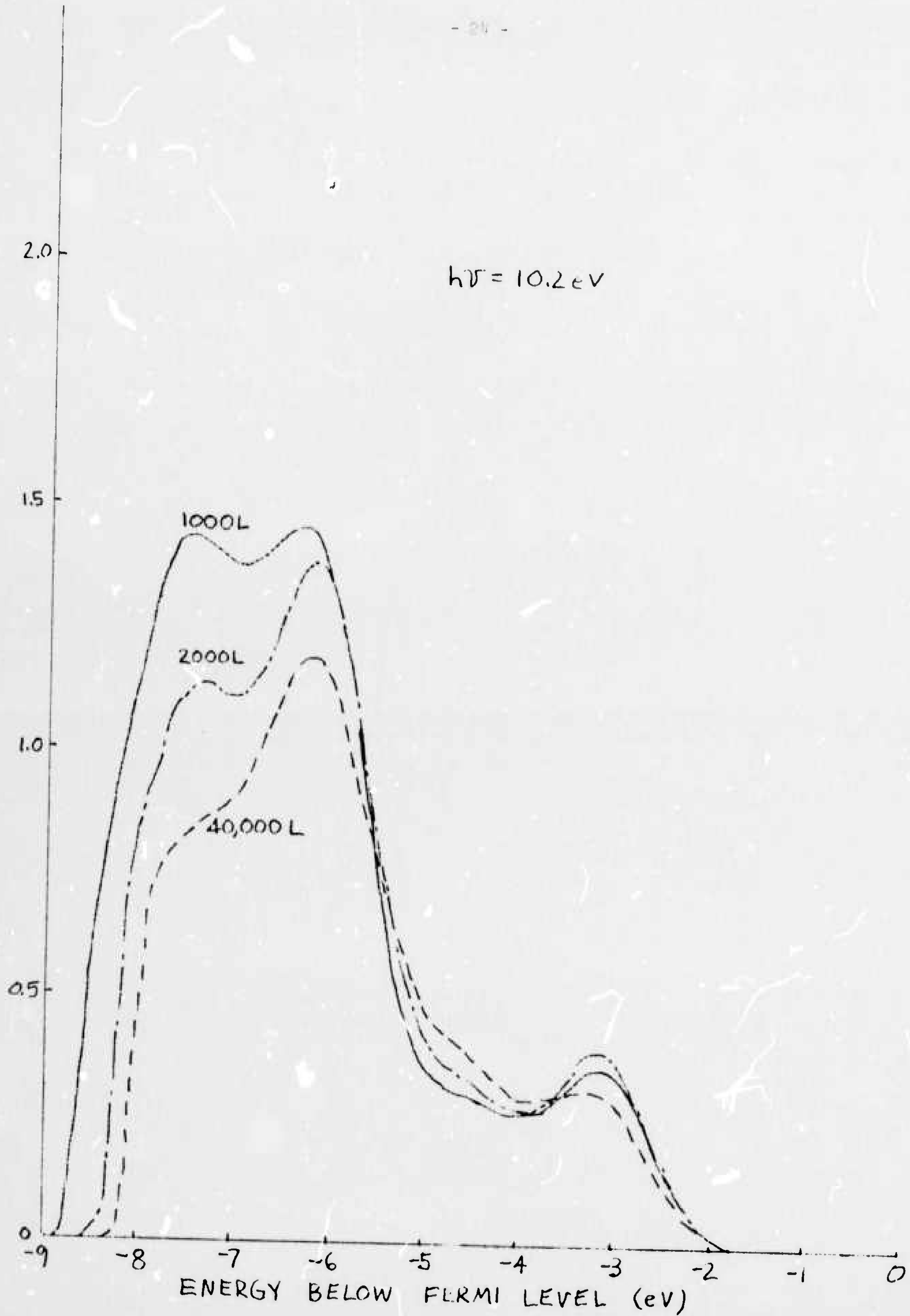

FIGURE 1

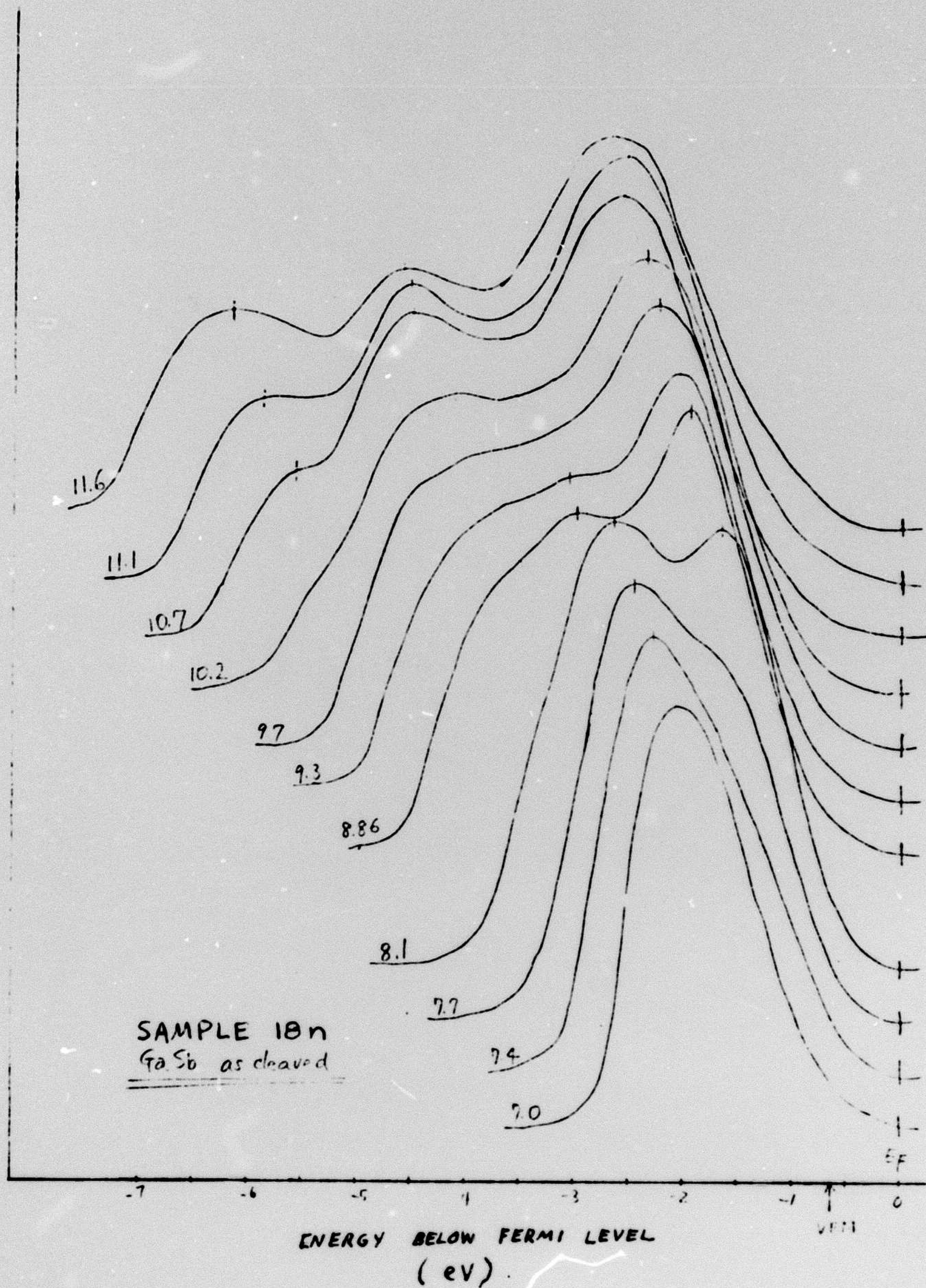

FIGURE 11

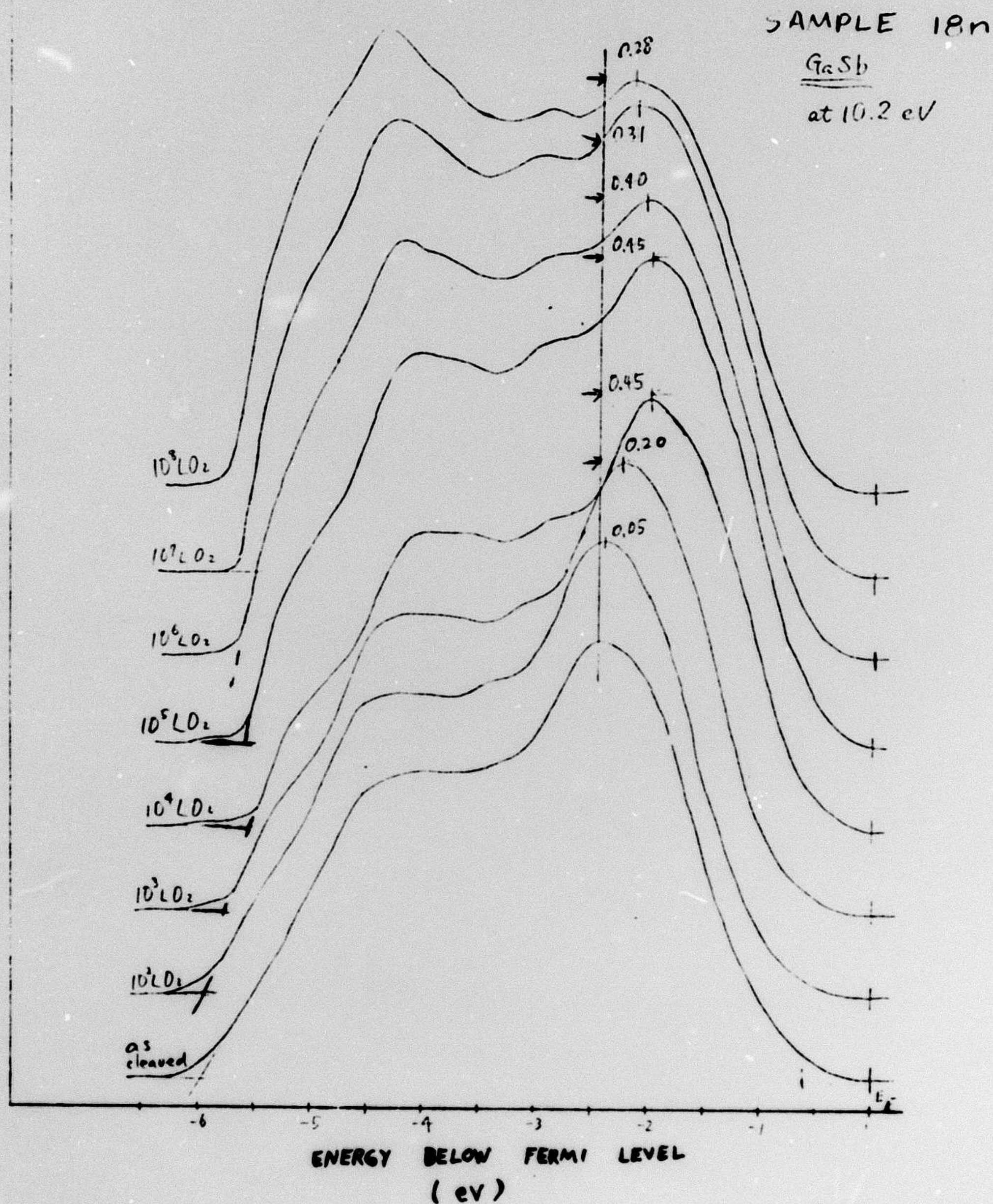

FIGURE 12

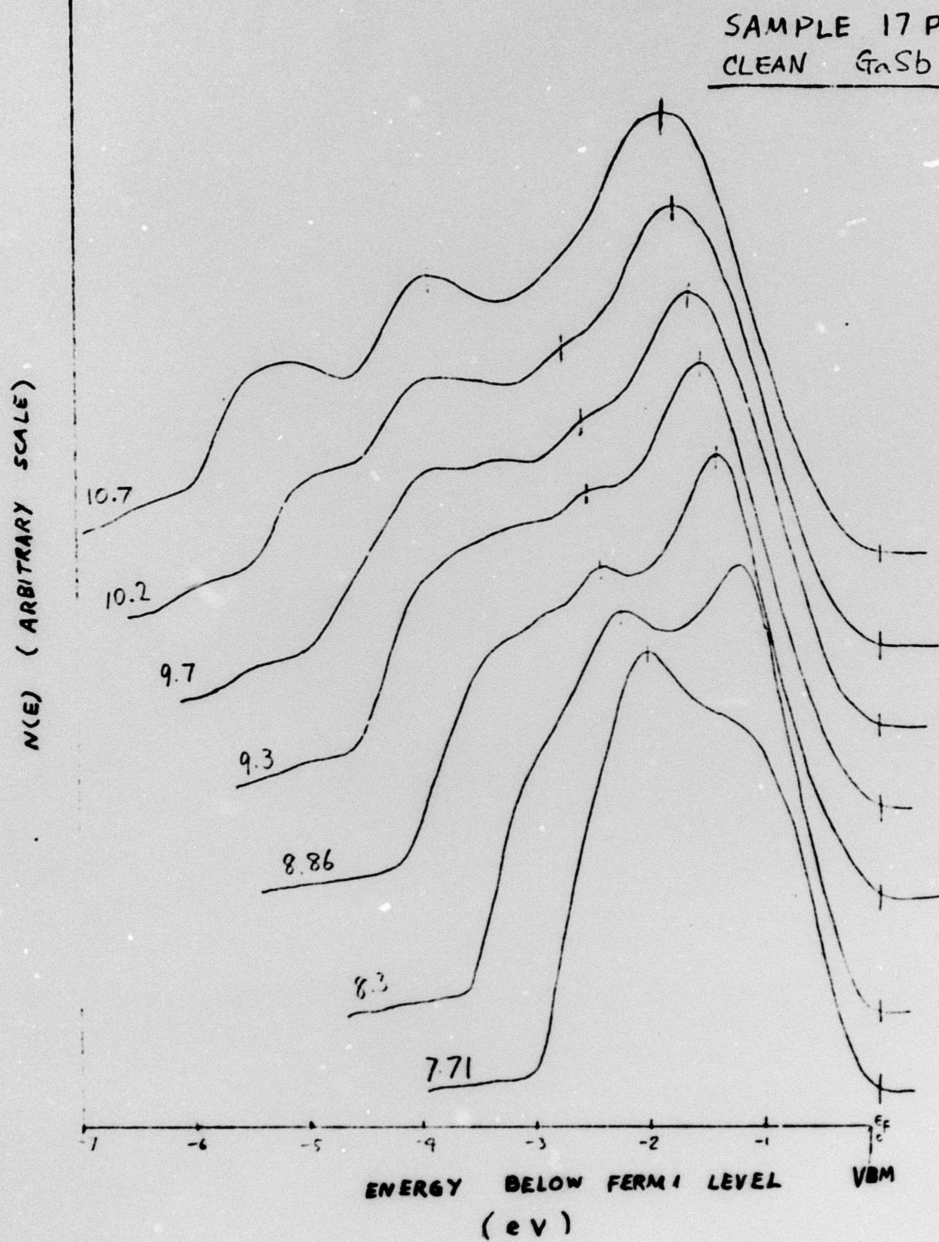

FIGURE 13

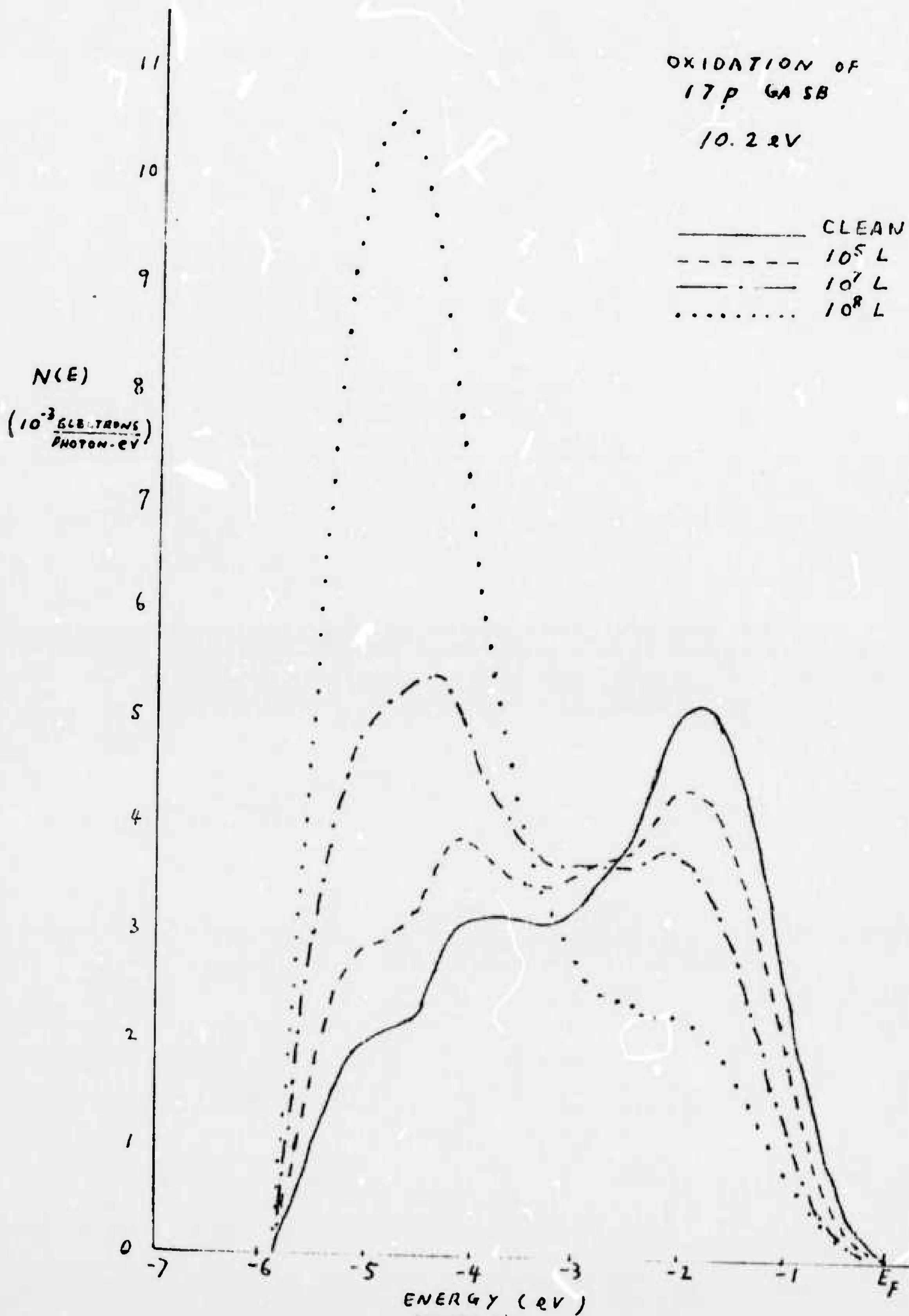

FIGURE 14

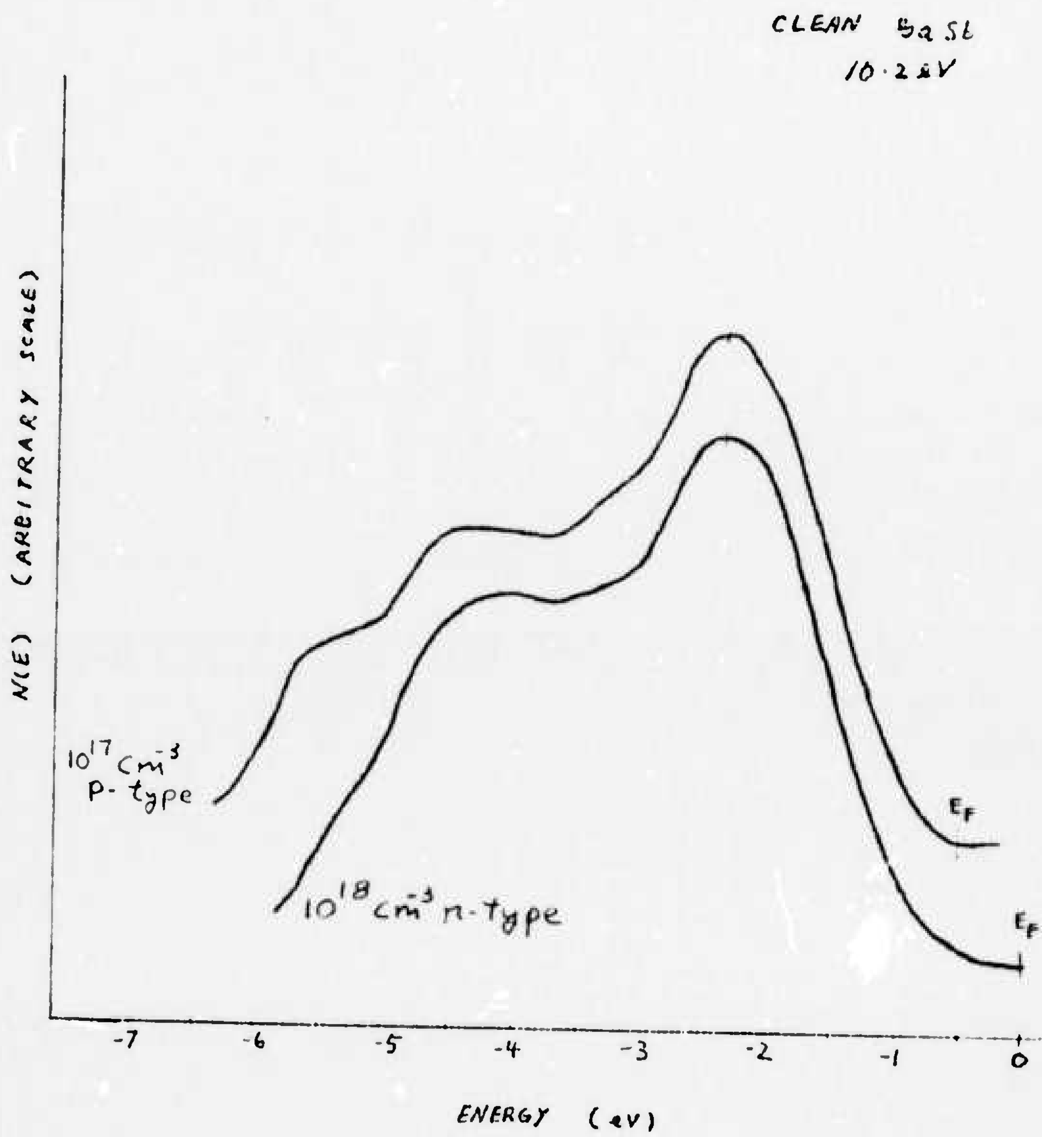

FIGURE 15

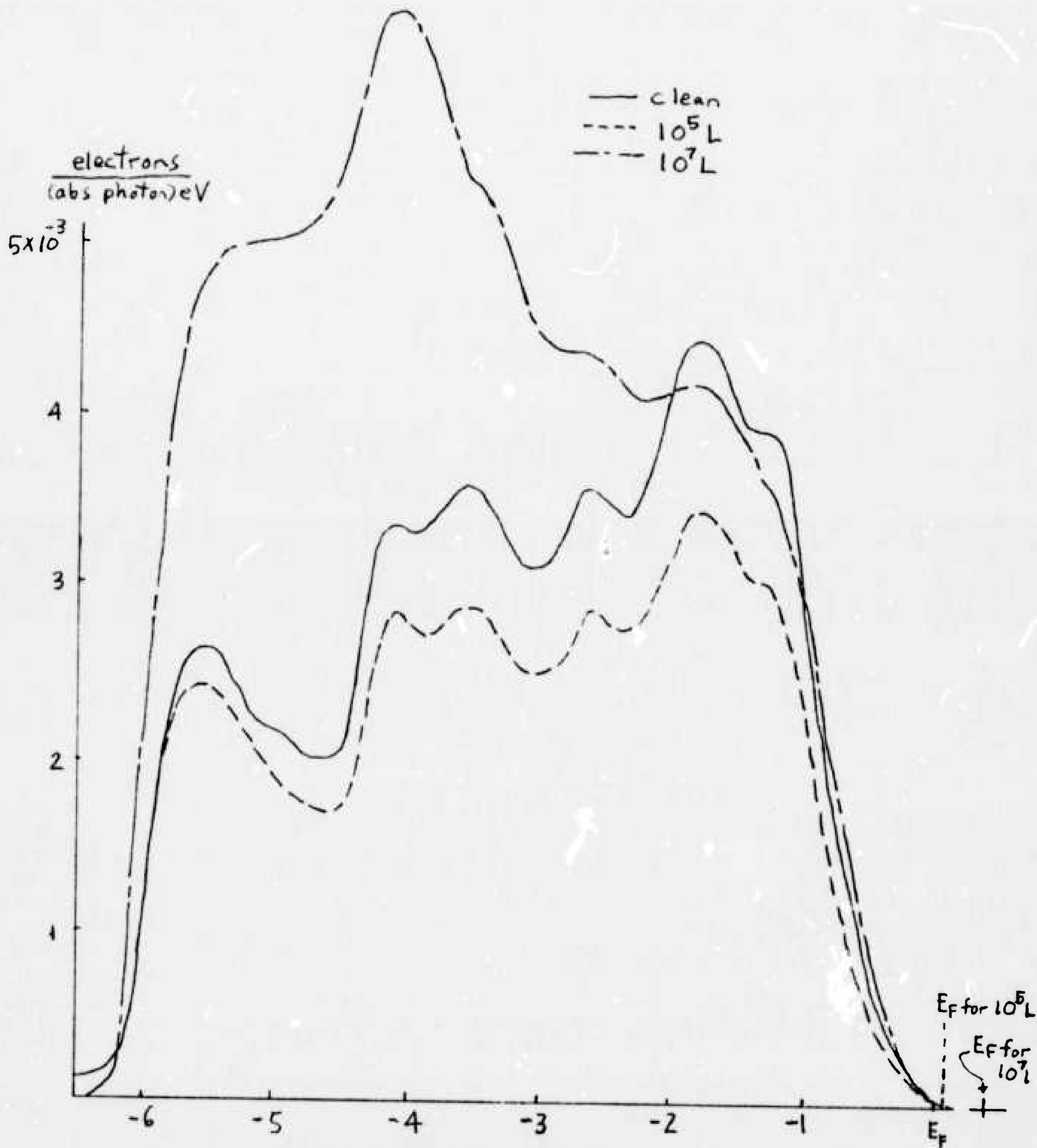

FIGURE 16

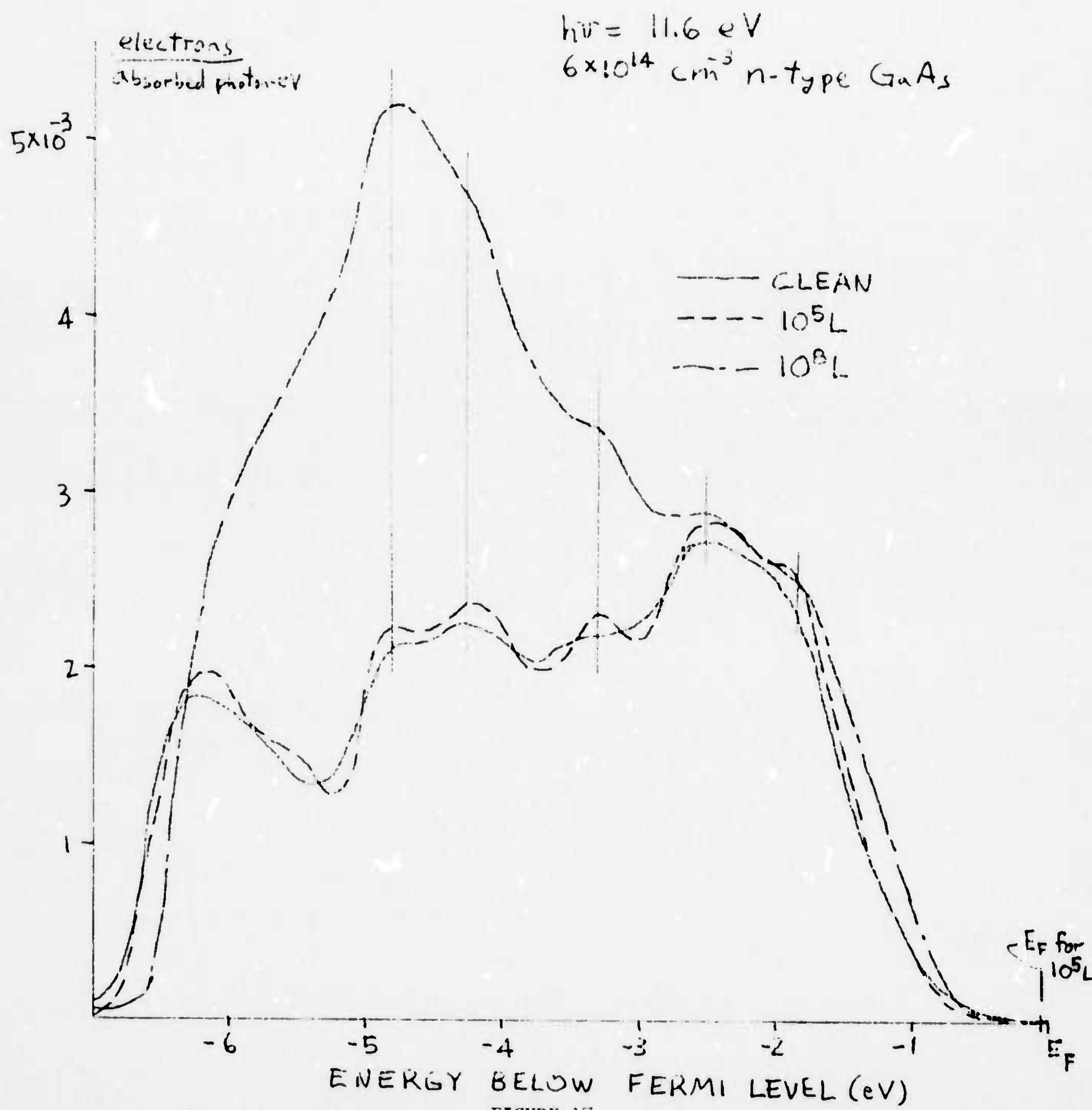

FIGURE 17

FIGURE 18

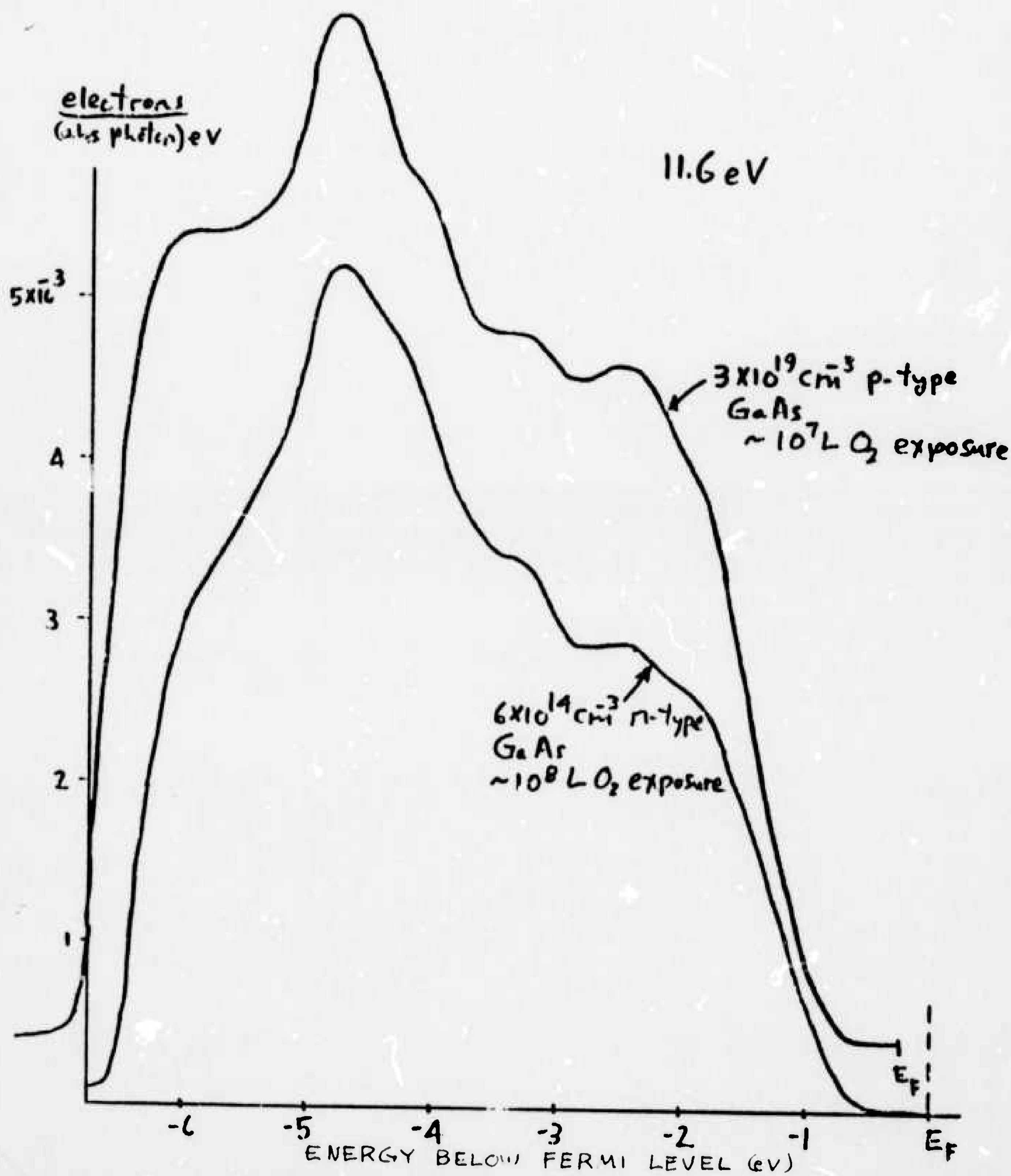

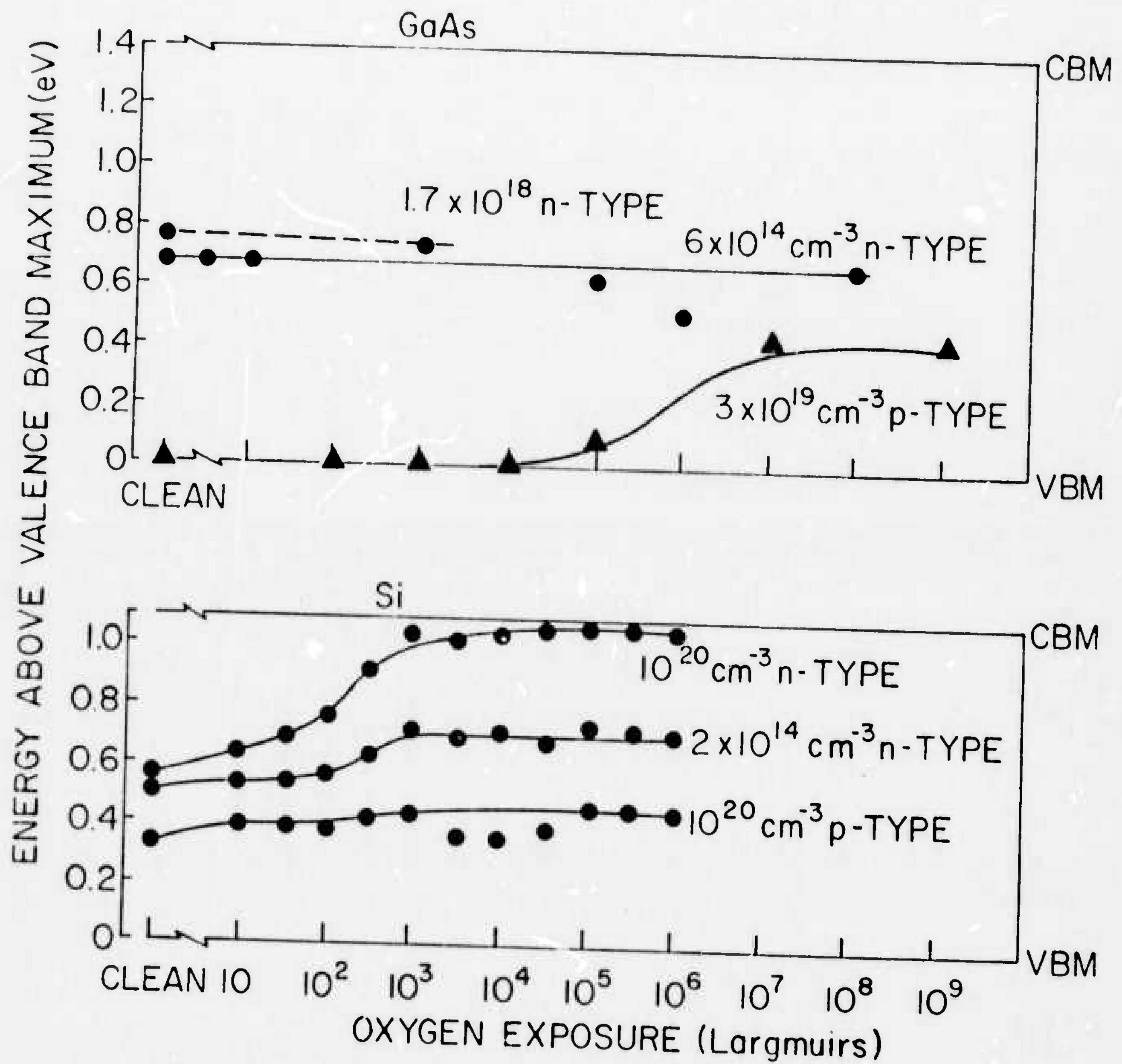

FIGURE 19